

1

.

2 .

3

:

T1, T2 : 7 , 1.5 T gadolinium , 3 .

:

7

,

/

T1

, T2 (1 )

. T1

(3 )

T1

T2

/

:

(germ cell tumor)

Dohke

2 (11), Yamashita

6

(1, 2),

5-15%

(4),

11

(2-4).

2

(13).

(1, 2, 5-8).

2%(4)

27%

(3).

가

(scintigraphy)

, <sup>131</sup>I

1989

9

(2, 4, 7, 9-16),

(2, 7, 11, 14-16)

7

(4, 7, 11, 13). Matsumoto

53.9 )

40-70 (

1

(7),

. 6 (palpitation), (chief complaint)

<sup>1</sup>  
가  
<sup>3</sup>

CA-125가 가

1998 9 4 1998 12 11

1.5-T

. T1

3 5-16 cm ( 9.7 cm ) .

[illegible]

T1  
 T2  
 (cut section) (Figs. 1-3). T1  
 가 가4  
 가 가3 (Fig. 2), 가1 (Fig.  
 3) T2  
 T1 4 3

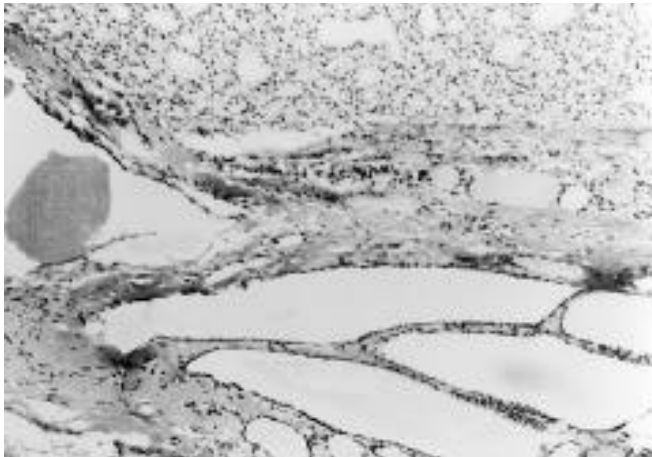
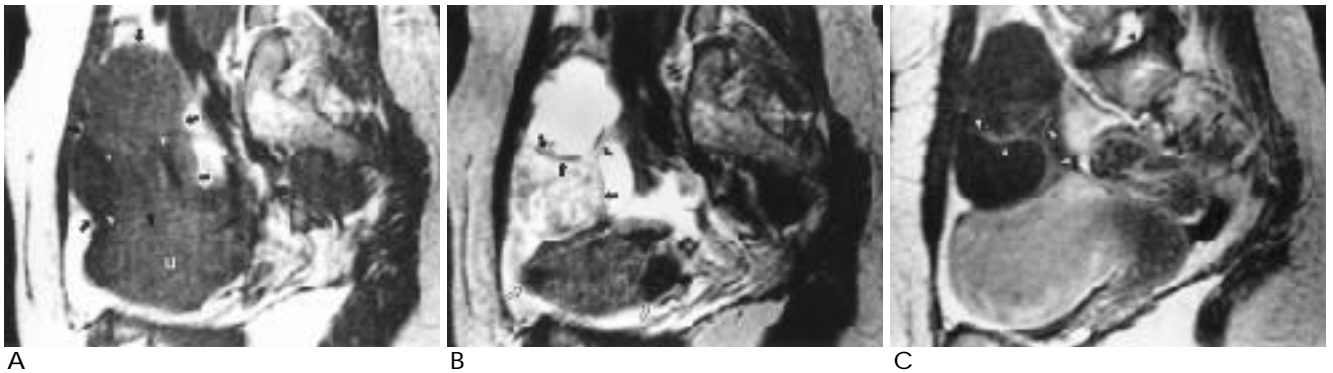


**Fig. 1. Sagittal pelvic MR images of right struma ovarii in a 73 year-old woman with preoperative diagnosis of an ovarian cancer (Case No. 1).**

A. T1-weighted image (TR/TE 500/16 msec) reveals a large complex pelvic mass (black arrows) of which signal intensity is mainly similar to that of the uterus (u). This mass also contains some hypointense strands (white arrowheads).

**B.** Fast spin echo T2-weighted image (TR/TE/ETL 4,000/102/8) demonstrates a multiloculated tumor of hyperintense cystic areas with some isointense solid portions and septae (black solid arrows), and hypointense uterine myomas (black open arrows).

C. Gadolinium enhanced sagittal T1 weighted image at the mid-line of the body reveals nonenhancing cystic contents of variable signal intensities with moderately enhancing solid portions and septae (white arrowheads) of the tumor.

D. Pathologic microscopy revealed that the mass was composed of thyroid tissue containing multiple follicles filled with eosinophilic viscous colloid.

Table 1. MRI Findings of Seven Cases of Pathologically Proven Struma Ovarii

No.	Age	Site	Size(cm)	T1WI		T2WI		Gd-T1WI	
				Cystic	Solid	Cystic	Solid	Cystic	Solid
1.	73	R	10 × 9 × 7	iso	iso	hyper	sl. hyper	UE	ME
2.	42	R	7 × 6 × 5	hypo	iso	hyper	sl. hyper	UE	IE
3.	65	L	10 × 8 × 5	iso	iso	hyper	sl. hyper	UE	IE
4.	57	R	12 × 11 × 9	hyper	iso	hyper	iso	UE	IE
5.	37	L	16 × 13 × 9	hypo	iso	hyper	iso	UE	IE
6.	40	R	5 × 4 × 2	iso	sl. hyper	hyper	iso	UE	IE
7.	63	L	8 × 5 × 3	hypo	iso	hyper	sl. hyper	UE	IE

MRI: magnetic resonance image, T1WI: T1-weighted image, T2WI: T2-weighted image, Gd-T1WI: gadolinium-DTPA enhanced T1-weighted image with or without fatsaturation, hyper: hyperintense, hypo: hypointense, iso: isointense with surrounding pelvic muscles, sl.: slightly, UE: unenhanced, IE: intense contrast enhancement, ME: moderate enhancement, LN: lymph nodes

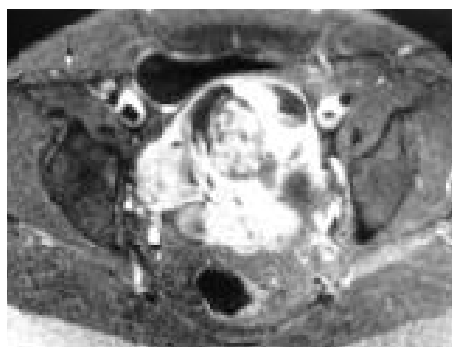
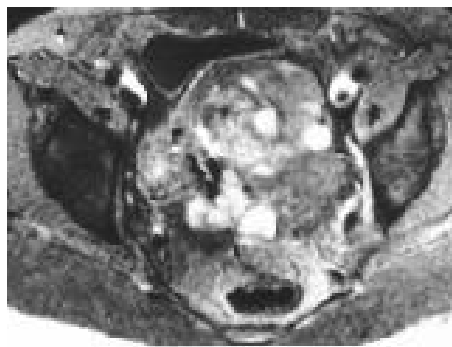
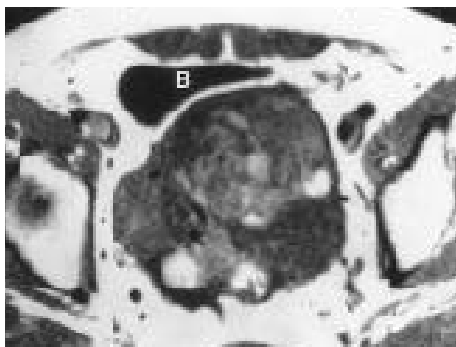


Fig. 2. Axial pelvic MR images of left struma ovarii in a 65 year-old woman with clinical impression of polycystic ovarian disease due to past medical history of primary infertility (Case No. 3).

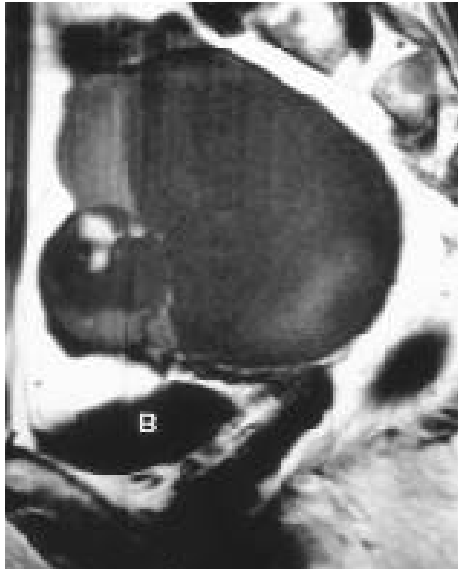
A. T1-weighted image (TR/TE 450/10) reveals a large complex pelvic mass of variable signal intensities behind the urinary bladder (B).

B. Fat saturated T1-weighted image (TR/TE 549/17) reveals that the hyperintense areas on T1 weighted image are not fatty tissue, because those areas are not suppressed as subcutaneous or pelvic fat.

C. Fast spin echo T2-weighted image (TR/TE/ETL 3,200/95/8) demonstrates a complex multiloculated mass with hyper- or hypointense cystic areas (which pathologically correspond to thyroid follicles including proteinaceous colloid) and isointense solid portions (arrows) relative to the uterine muscle layer (u).

D. Fat saturated gadolinium enhanced

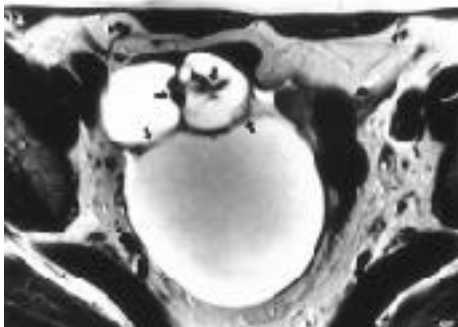
T1 weighted image (TR/TE 450/16) shows nonenhancing cystic contents and intensely enhancing solid portions and septae of the tumor. Pathologically, the solid parts of the tumor corresponded to the thyroid tissues composed of multiple follicles and stroma containing focal calcifications, abundant blood vessels and fibrous tissue, which might account for marked contrast enhancement. Focal calcifications were not distinct on all MR images.



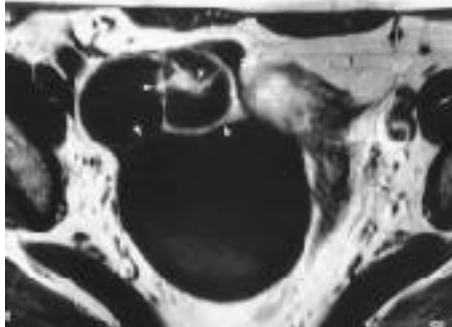
A



B



C



D

Fig. 3. Pelvic MR images of right struma ovarii in a 57 year-old woman with preoperative diagnosis of a mucinous ovarian cystadenocarcinoma (Case No. 4).

A. Sagittal T1-weighted image (TR/TE 420/14) demonstrates a large multiloculated mainly cystic pelvic mass of variable signal intensities above the urinary bladder (B).

B. Fat suppressed axial T1-weighted image (TR/TE 600/14) reveals the non-fatty nature of the cystic contents of the mass.

C. Fast spin echo axial T2-weighted image (TR/TE/ETL 3,800/132/8) demonstrates that the mass is composed of hyperintense fluid and isointense solid portions and septae (arrows) relative to the pelvic muscles.

D. Gadolinium enhanced axial T1-weighted image (TR/TE 440/14) shows nonenhancing cystic contents and intensely enhancing solid portions and septae (white arrowheads) of the tumor. Pathologically, the cysts were filled with gelatinous fluid of eosinophilic colloid and some hemorrhagic products, and the solid portions of the tumor consisted of thyroid tissues.

(4 , ) (3 ) 7  
(Figs. (viscous)  
(eosinophilic)  
T1  
T2 /  
T1  
(Figs. 1-3).  
( 0.7-4.8 cm)  
가 가 3 )  
1 (3 )  
(Fig. 2). 1 cm  
(4, 5 ) (4 ) 7  
- 7  
(7 )  
) 가  
가 , 1 (4 )

(4, 7, 11, 13) 가 .

(multilocularity)

(monodermal) (highly specialized)

가 (4, 7, 11, 13)

(carcinoid) (17).

2.7%

가

(3, 18, 19), 0.3% (7, 18).

가

85%

가 T1 / /

(2, 20, 21), 4

7 40-70 ( 53.9 )

가 20-44 (22, 23)

. T1

(24), 가 4 , T2 (chemical shift)가

가

T1 , T2

(2, 7, 25).

(4, 7, 11, 13) . Dohke 2

T1 /

“가 (pseudo) Meigs

(3, 4),

가

(11).

(4, 7, 11, 26)

(3), 5-10%

(2, 24). 7

(total abdominal hysterectomy)

6 -9

가

0.3%

가 (19)

, T1

가

(2, 7,

11) (4, 9, 10, 12, 13).

(4, 7,

가

11, 13). , Matsumoto

1 (7), Dohke

2 (11), Yamashita 6

가 (4),

11 2

(13).

S-

가 (shading artifact)

가

가  
가  
가 , 7 가  
가  
가  
T1  
T2 /  
가  
가

1. Fox H, Langley FA. *Tumors of the ovary*. London: Heineman, 1976;240-245
2. March DE, Desai AG, Park CH, Hendricks PJ, Davis PS. Struma ovarii: hyperthyroidism in a postmenopausal woman. *J Nucl Med* 1988;29:263-265
3. Talerma A. *Germ cell tumors of the ovary*. In Kurman RJ, ed. Blaustein's pathology of the female genital tract. 3rd ed. New York, NY: Springer-Verlag, 1987:687-721
4. Yamashita Y, Hatanaka Y, Takahashi M, Miyazaki K, Okamura H. Struma Ovarii: MR appearances. *Abdom Imaging* 1997;22:100-102
5. Thomas RD, Batty VB. Metastatic malignant struma ovarii. *Clin Nucl Med* 1992;17:577-578
6. Radecki PD, McKrisky PJ. *Female Pelvis: neoplastic and nonneoplastic masses*. In Friedman AC, Radecki PD, Lev-Toaff AS, Hilpert PL, eds. *Clinical pelvic imaging*. St. Louis: the C.V. Mosby company, 1990:197-204
7. Matsumoto F, Yoshioka H, Hamada T, Ishida O, Noda K. Struma ovarii: CT and MR findings. *J Comput Assist Tomogr* 1990;14(2):310-312
8. Ayhan A, Yanik F, Tuncer R, Tuncer ZS, Ruacan S. Struma ovarii. *Int J Gynaecol Obstet* 1993;42:143-146
9. Kozuka Y, Tamaishi Y, Yamawaki T, Sugiyama Y. A case of struma carcinoid. *Obstet Gynecol* 1983;50:1991-1994
10. Hahn ST, Park SH, Bahk YW, Chung SK. Struma ovarii simulating

a teratodermoid cyst: computed tomographic findings in one case. *Radiologie* 1991;31:89-91

11. Dohke M, Watanabe Y, Takahashi A, et al. Struma ovarii: MR findings. *J Comput Assist Tomogr* 1997;21(2):265-267
12. Zale Y, Caspi B, Tepper R. Doppler flow characteristics of dermoid cysts: unique appearance of struma ovarii. *J Ultrasound Med* 1997;16(5):355-358
13. 1997;36:133-140
14. Thomas RD, Batty VB. Metastatic malignant struma ovarii: two case reports. *Clin Nucl Med* 1992;17:577-578
15. Lieberman G, Buscombe JR, Hilson AJ, Thakrar D, MacLean A. The detection of struma ovarii in two patients by radioimmunosintigraphy. *Am J Obstet Gynecol* 1998;179:262-263
16. Bayot MR, Chopra JJ. Coexistence of struma ovarii and Graves' disease. *Thyroid* 1995;5:469-471
17. Cotran RS, Kumar V, Robbins SL. *Female genital tract*. In Cotran RS, Kumar V, Robbins, SL, eds. *Robbins pathologic basis of disease*, 4th ed. Philadelphia: W.B. Saunders 1989:1127-1180
18. Stevens SK. *The adnexa*. In Higgins CB, Hricak H, Helms CA, *Magnetic resonance imaging of the body*, 2nd ed. New York: Raven Press, 1992:875-877
19. Gusberg SB, Danforth DN. Clinical significance of struma ovarii. *Am J Obstet Gynecol* 1944;48:532-542
20. Sciarra JJ. *Benign neoplasm of the ovary*. In Bird CC, McElin TW, Victor TA, eds. *Gynecology and obstetrics*. Philadelphia: JB Lippincott, 1988;12
21. Fox JF, Clement KW. Functioning struma ovarii. *Ann Surg* 1951;133:253-254
22. Griffiths CT, Berkowitz RS. *The ovary*. In Kistner RW, ed. *Gynecology: principles and practice*. St. Louis: Mosby-year book, inc., 1986:173-175
23. Scoult LM, McCarthy SM. *Female pelvis*. In Stark DD, Bradley WG, eds. *Magnetic resonance imaging*. 2nd ed. St. Louis: Mosby-year book, inc., 1992:1973-1976
24. Marcus CC, Marcus SL. Struma ovarii: a report of 7 cases and a review of the subject. *Am J Obstet Gynecol* 1961;81:752-761
25. Szyfelbein WM, Young RH, Scully RE. Cystic struma ovarii. A frequently unrecognized tumor. A report of 20 cases. *Am J Surg Pathol*. 1994;18:785-788
26. Smith FG. Pathology and physiology of struma ovarii. *Arch Surg* 1946;53:603-626

## MR Findings of Struma Ovarii<sup>1</sup>

Jong Chul Kim, M.D., Jae Young Byun, M.D.<sup>2</sup>, Young Rae Lee, M.D.<sup>3</sup>

<sup>1</sup>Department of Diagnostic Radiology, Chungnam National University School of Medicine

<sup>2</sup>Department of Diagnostic Radiology, Kangnam St Mary's Hospital, Catholic University Medical College

<sup>3</sup>Department of Diagnostic Radiology, Kangbuk Samsung Hospital, Sungkyunkwan University College of Medicine

**Purpose :** To characterize the magnetic resonance (MR) findings of struma ovarii, a rare ovarian tumor composed solely or predominantly of thyroid tissue or the tumor in which hyperthyroidism results from the ovarian thyroid tissue.

**Materials and Methods :** In seven patients, MR images (T1-weighted with or without gadolinium enhancement and T2-weighted) were obtained in the axial, coronal, and sagittal planes using 1.5-T MR units, and in three of seven patients the fat saturation technique were performed. MR findings were retrospectively evaluated for the site, size, components, signal intensity, presence and degree of contrast enhancement, and associated findings. These and pathologic findings were compared.

**Results :** MR images showed unilateral complex masses composed of multiple cysts and some solid components, corresponding pathologically to thyroid follicles containing colloid and the stroma with abundant blood vessels and fibrous tissue. Cystic portions of the tumors had variable signal intensities on T1-weighted images, and high signal intensities on T2-weighted images. Some hyperintense cystic areas seen on T1-weighted images were due to hemorrhage (n= 1) and colloid components (n= 3). Solid portions of the tumors were isointense relative to adjacent muscles (with intense contrast enhancement), as seen on T1-weighted images, and iso- or hyperintense on T2-weighted images.

**Conclusion :** Struma ovarii has a characteristic MR appearance of a complex mass composed of multiple cysts and intensely enhanced solid components.

**Index words :** Ovary, neoplasms

Ovary, cysts

Ovary, MR

Address reprint requests to : Jong Chul Kim, M.D., Department of Diagnostic Radiology, Chungnam National University School of Medicine,  
#640 Daesa-dong, Jung-ku, Taejeon, 301-040, Korea.  
Tel. 82-42-220-7835 Fax. 82-42-253-0061